Disentangling interfacial redox processes of proteins by SERR spectroscopy

Daniel H. Murgida*[a] and Peter Hildebrandt*[b]

Surface-enhanced resonance-Raman spectroelectrochemistry represents a powerful approach for studying the structure and reaction dynamics of redox proteins immobilized on biocompatible electrodes in fundamental and applied sciences. Using this approach it has been recently shown that electric fields of biologically relevant magnitude are able to influence crucial parameters for the functioning of a variety of soluble and membrane bound heme proteins. Electric field effects discussed in this *tutorial review* include modulation of redox potentials, reorganization energies, protein dynamics and redox-linked structural changes.

1 Introduction

Resonance-Raman (RR) spectroscopy is nowadays a well established technique that is part of the tool box of biophysical chemists. Compared to infrared absorption, this method possesses a couple of distinct features that make it particularly suitable for studying structure–function relationships in biomolecules, especially metalloproteins. First, the biological solvent, water, and most biologically relevant buffers present extremely weak Raman activity. Second, measurements can be done with intramolecular selectivity by simply tuning the excitation laser in electronic resonance with a chromophore of the biomacromolecule, *e.g.* a cofactor or an aromatic amino acid in a protein. This resonance enhancement, which can achieve several orders of magnitude, also provides high sensitivity.[1,2] For example, the active site of a heme enzyme can easily be studied at sub-micromolar levels without interference of the protein matrix or the solvent. Indeed, RR spectroscopy

has been extensively used for characterizing a large variety of soluble and membrane-bound proteins including one or more heme prosthetic groups of different types and coordination patterns, as well as model compounds.[3–5] Perhaps the best studied heme protein is cytochrome *c* (Cyt-*c*) whose RR spectrum was fully assigned by Hu *et al.*[6] providing a solid basis for the interpretation of RR spectra of heme proteins in general.

Soon after the discovery of the surface-enhancement effect, Cotton, Schultz and Van Duyne[7] pioneered its combination with the electronic resonance enhancement for studying proteins adsorbed on metal surfaces. The resulting technique, surface-enhanced resonance-Raman (SERR), presents unsurpassed sensitivity and selectivity among vibrational methods.[8] Severe drawbacks, however, are denaturation of biological macromolecules by interactions with the metal substrate and enhanced laser-induced degradation of the adsorbed species. These problems have been overcome with the development of biocompatible coatings, the design of more suitable sampling devices, and the advent of more sensitive detectors that allow the use of low laser powers and short acquisition times.

For example, rotating silver ring electrodes with nanostructured surfaces and coated with self assembled monolayers (SAMs) of ω-functionalized alkanethiols represent an ideal platform for studying heme redox proteins with SERR

[a] *Departamento de Química Inorgánica, Analítica y Química Física/INQUIMAE-CONICET. Facultad de Ciencias Exactas y Naturales, Universidad de Buenos Aires. Ciudad Universitaria Pab. 2, piso 1, C1428EHA-Buenos Aires, Argentina. E-mail: dhmurgida@qi.fcen.uba.ar*
[b] *Technische Universität Berlin, Institut für Chemie, Sekr. PC14, Straße des 17. Juni 135, D-10623 Berlin, Germany. E-mail: hildebrandt@chem.tu-berlin.de*

Daniel H. Murgida is a Chemistry Professor and CONICET Researcher at INQUIMAE, University of Buenos Aires and a Visiting Professor at the Institute of Chemical and Biological Technology (ITQB, Universidade Nova de Lisboa). His main research interests involve electron-transfer proteins and biological photoreceptors.

Peter Hildebrandt is a Full Professor for Physical Chemistry and Biophysical Chemistry at the Technische Universität Berlin and Visiting Professor at ITQB. His current research interests cover biological electron transfer processes, reactions at interfaces, and molecular processes of photoreceptors. The methodological toolbox includes various vibrational spectroscopic techniques, complemented by theoretical approaches.

detection under controlled potentials. Moreover, time-resolved SERR spectroelectrochemistry allows the simultaneous monitoring of protein dynamics, structural changes and electron transfer reactions over a broad time scale.[9-11]

Most heme redox proteins exert their natural function at biological membranes. Typical examples are respiratory and photosynthetic chains where a number of soluble and membrane-bound heme-containing proteins intervene in electro-protonic energy transduction. All these processes occur under the influence of strong electric fields brought about by transmembrane, dipole and surface potentials. SAM-coated electrodes are able to mimic some of the basic features of biological membranes, including controlled electric fields of biologically relevant magnitude.

This tutorial review will highlight recent developments and perspectives in the study of electron transfer dynamics of heme proteins by stationary and time-resolved SERR spectroelectrochemistry with special emphasis on electric field effects.

2 Surface-enhanced resonance-Raman scattering of heme proteins

Since the transition dipole moments of hemes lie in the porphyrin plane, resonance enhancement is only expected for the *gerade* in-plane vibrational modes. Upon Soret-band excitation the RR spectrum is dominated by the totally symmetric modes A_{1g} which gain intensity *via* the A-term enhancement mechanism. These bands lose intensity upon Q-band excitation and instead the non-totally symmetric modes B_{1g}, A_{2g} and B_{2g} gain intensity through the B-term enhancement mechanism (Fig. 1).[2,5,6]

These considerations assume an idealized D_{4h} symmetry for the porphyrin. The lower symmetries that characterize asymmetrically substituted hemes can induce RR activity of other modes, although the general conclusions are still valid.

Vibrational modes in the so-called marker band region (*ca.* 1300–1700 cm^{-1}) are largely composed by C–C and C–N
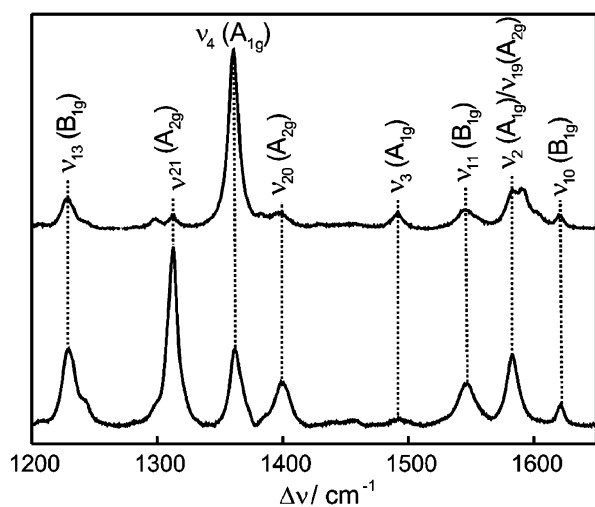
Fig. 1 Resonance-Raman spectra of ferrous Cyt-*c* measured under Soret (top) and Q-band (bottom) excitation. Bands are labeled according to Hu *et al.*[6]
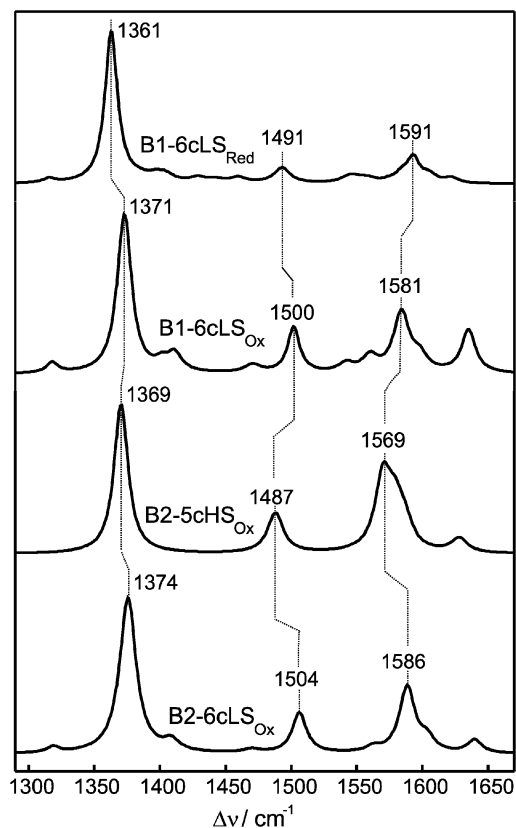
Fig. 2 RR component spectra of native (B1) and non-native (B2) forms of Cyt-*c*. See text for details.

stretching vibrations of the porphyrin. In particular, the most prominent band, ν_4, is a nearly pure C–N stretching. Therefore, the position of this band is extremely sensitive to the redox state of the protein (Fig. 1) due to the increased electron back donation of Fe^{2+} compared to Fe^{3+} into the π^* orbital of the porphyrin, which weakens the C–N bonds. In general terms, this and most of the other bands in the high frequency region are sensitive markers not only of the redox state but also of the spin and ligation pattern of the heme iron. For example, Fig. 2 shows the component spectra for the ferrous and ferric forms of native Cyt-*c* which possess a six-coordinated low-spin iron (B1-6cLS$_{Red}$ and B1-6cLS$_{Ox}$, respectively) as well as two non-native ferric forms in which the sixth natural ligand Met80 is missing and the position remains either vacant or occupied by a histidine residue (B2-5cHS$_{Ox}$ and B2-6cLS$_{Ox}$, respectively).[12]

In this specific case, given that the spectral components and the relative RR cross sections are known, structural equilibria can be quantitatively analyzed by simulating the experimental spectra on the basis of the component spectra of the species involved, using solely their relative weights as adjustable parameters.[13] Relative concentrations determined in that way may have an accuracy better than 5%, depending on the spectral quality and the number of coexisting species.

The low-frequency region, particularly below 500 cm^{-1} (not shown), includes modes with significant contributions from the porphyrin substituents and, therefore, reflect protein–cofactor interactions.

When the protein is adsorbed on a surface-enhanced Raman (SER) active substrate the electric field component of the exciting laser beam interacts with the surface plasmons of the metal substrate amplifying the local field and thus intensifying the Raman spectrum. Enhancement is achieved *via* the individual components of the scattering tensor depending on the direction of the electric field vector and the orientation of the heme plane with respect to the surface.[8] Assuming a D_{4h} porphyrin symmetry, one can anticipate that the A_{1g} modes will experience preferential enhancement when the heme plane is parallel to the surface, while for a perpendicular orientation A_{1g}, A_{2g}, B_{1g} and B_{2g} modes will all be enhanced.[14,15] Therefore, different orientations of the adsorbed protein are expected to lead to different intensity ratios of modes of different symmetries, *e.g.* $\nu_{10}(B_{1g})/\nu_4(A_{1g})$.

An accurate quantitative determination of the orientation parameters is usually precluded by the nano-topography of the SER substrate and differential enhancements at different points of the nano-structured surface. The situation is aggravated when the measurements are performed under strong electronic resonance, *e.g.* under Soret band excitation, due to enhanced depolarization of the scattered radiation. Thus, surface-enhanced resonance-Raman (SERR) spectra of heme proteins measured at *ca.* 410 nm excitation are essentially identical to their RR in solution in terms of band positions, widths and relative intensities. This can be seen as a disadvantage or as a good opportunity. Using Ag substrates and violet excitation one can achieve simultaneously maximum resonance enhancement due to the strong electronic absorption of the heme and maximum surface enhancement due to the strong coupling of the laser radiation with the surface plasmons of this metal. The overall enhancement factors with respect to standard Raman measurements can achieve several orders of magnitude, usually more than 10. Indeed, excellent spectra can be obtained under Soret excitation at sub-monolayer protein coverage. Furthermore, SERR spectra are directly comparable to RR spectra of the native protein in solution facilitating spectral analysis and structural interpretation.[9–11]

Excitation in resonance with the much weaker Q electronic band of hemes (*ca.* at 514 nm) leads to an intermediate situation. Depolarization of the scattered radiation is still appreciable but not complete. Thus, although absolute orientations can not be accurately determined, changes of average orientations can still be observed providing the basis for the direct monitoring of protein dynamics at interfaces (*vide infra*).[16]

In summary, SERR spectroscopy is able to monitor the redox state, structural features and orientation of heme proteins immobilized on metal electrodes with unsurpassed sensitivity, thereby constituting a powerful detection method for spectroelectrochemical studies.

3 Biocompatible immobilization of proteins

It has been early recognized that direct adsorption of proteins to nano-structured metal substrates often leads to partial protein unfolding and, eventually, to complete denaturation.[17] Therefore, metal substrates are coated with organic films of different chemical nature in order to provide a biocompatible interface for subsequent protein immobilization. For SERR spectroelectrochemical applications an additional requirement to be fulfilled is that the immobilization strategy must ensure efficient electronic communication between the metal electrode and the redox center of the protein. Most soluble redox proteins are small in size and act as electron carriers between large membrane bound protein complexes and have, therefore, redox sites which are partially exposed or very close to the surface. Moreover, the region of the partially exposed redox center is structurally optimized for recognition by the reaction partner in order to form a transient complex that precedes electron transfer. Thus, the simplest approach is to prepare coatings that mimic the interactions within the protein–protein complexes. Electron flow between the electrode and the immobilized protein then proceeds *via* the superexchange mechanism, involving through-bond and, eventually, through-space tunnelling across the coating.[18]

For the most widely used SER/SERR substrates, Ag and Au, surface modification is most easily achieved by chemisorption of thiols, disulfides or dithiolanes. When bound to a relatively long alkyl chain, these compounds form densely packed self-assembled monolayers to which proteins can be anchored in different ways depending on the functional tail groups of the alkanethiols and the surface properties of the proteins.[11] Moreover, the same protein can be immobilized in different manners. For example, ω-carboxylalkanethiols (COOH-SAMs) are often used for the electrostatic adsorption of Cyt-*c*[19–22] which has a ring-shaped arrangement of positively charged residues around the partially exposed heme and a large dipole moment. However, Cyt-*c* can also be immobilized on CH_3-terminated SAMs (CH_3-SAMs) *via* hydrophobic interactions with the central patch around the partially exposed heme.[23] Alternatively, the protein can be covalently linked to COOH- and NH_2-terminated SAMs using cross linking reagents[24] or coordinatively bound to alkanethiols containing a functional group, *e.g.* pyridinyl, able to displace the weakly bound methionine axial ligand of the heme iron.[25,26]

Similar strategies, including mixed SAMs, have been applied to a variety of soluble redox proteins, including cytochromes P450,[27] b_{562},[28] c_3,[29] c_6,[30] azurin[31] and Cu_A centers.[32,33]

Frequently, the motivation for biocompatible protein immobilisation is the fabrication of bioelectronic devices, *e.g.* sensors, that take advantage of the unique properties of redox proteins and enzymes in terms of specificity, recognition or catalytic activity. In these cases, in order to increase the sensitivity, it is crucial to achieve a protein load on the electrode surface that goes well beyond the monolayer level, the limit when using simple alkanethiol SAMs. A popular way to overcome that limit consists in layer-by-layer deposition of conductive polyelectrolytes, such as poly(anilinesulfonic acid), and the protein of interest.[34,35] Alternatively, the electrode surface can be nanostructured in such a way that the surface area is significantly increased allowing for a substantial protein load even using the conventional SAM-coating techniques for subsequent immobilization of a protein monolayer. A recent example is the electrodeposition of coral-like Ag

This journal is © The Royal Society of Chemistry 2008

Chem. Soc. Rev., 2008, **37**, 937–945 | 939
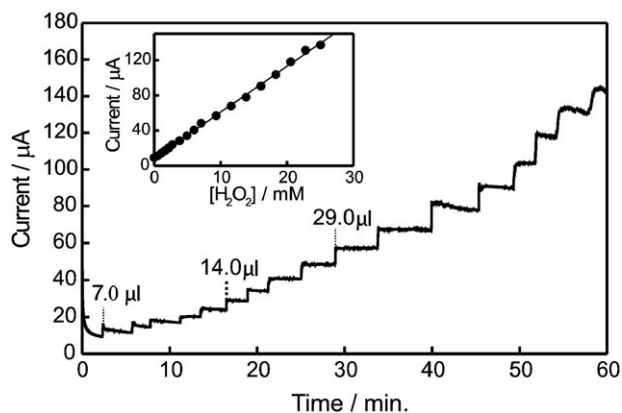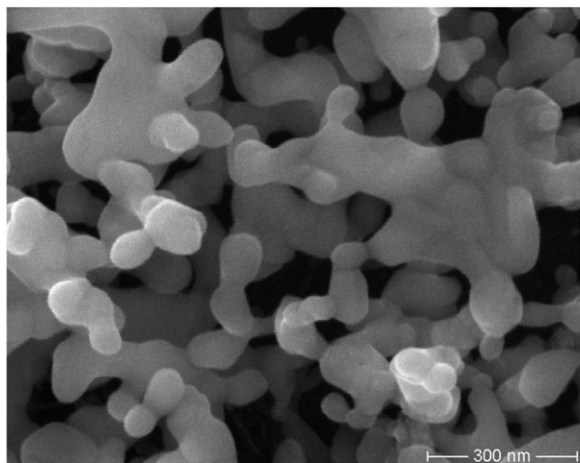
Fig. 3 Top: SEM image of a silver nanocoral electrode. Bottom: Amperometric response of a nanocoral/SAM/Cyt electrode at −100 mV upon successive additions of different volumes of 5 mM H_2O_2 to the electrochemical cell. The inset shows the linear response of the electrocatalytic current with H_2O_2 concentration.

nanostructures on graphite electrodes using detergents to direct crystal growth (Fig. 3).[36]

Nanocorals, which present outstanding SERR activity, were subsequently coated with mercaptohexanoic acid for the electrostatic adsorption of Cyt-*c*. Using SERR and electrochemical methods it was shown that the strategy leads to a surface concentration equivalent to 50 fully packed monolayers of native and electroactive protein. The devices were proven to be excellent H_2O_2 sensors (Fig. 3), with remarkably broad dynamic range, high sensitivity, good reproducibility and reusability.[36]

In the case of integral membrane proteins, a specific requirement for immobilization is the preservation of a hydrophobic environment either by a lipid bilayer membrane or a solubilizing detergent. Electrochemical communication is a particularly challenging task due to the size of the complexes and deep embedment of the redox sites within them.

For robust membrane proteins, the simplest possible immobilization procedure consists in the direct adsorption of the detergent-solubilized complex on the bare electrode. The underlying principle is that the solubilizing detergent adsorbs on the metal providing a biocompatible interface. This method was successfully applied to the *aa*₃ quinol oxidase from

Acidianus ambivalens, which could be directly adsorbed on a bare nanostructured Ag electrode under preservation of the native structure.[37] The adsorbed *aa*₃ enzyme presents good electrochemical response that allowed the unambiguous determination of midpoint potentials for the individual hemes from SERR potentiometric titrations. A very interesting feature from this study is that the midpoint potentials for hemes *a* and *a*₃ are reversed and not subjected to significant Coulombic interactions compared to the mitochondrial-like *aa*₃ enzymes, implying a different electroprotonic energy transduction mechanism.

Detergent-assisted direct adsorption, however, does not work for more fragile membrane proteins. An alternative approach is based on tethering the solubilised protein *via* a histidine-tag to an electrode functionalized with nickel nitrilotriacetate (Ni-NTA) and subsequent replacement of the detergent by phospholipids to reconstitute a quasi-natural membrane environment. This strategy has been applied for the immobilization of the *aa*₃ cytochrome *c* oxidase from *Rhodobacter sphaeroides*[38] and the *cbb*₃ enzyme from *Bradyrhizobium japonicum*.[39] A comparison of SERR and RR spectra indicate that indeed the immobilized proteins retain their native structures. Electronic communication with the metal substrate, however, is poor as indicated by the selective reduction of heme *a* for different constructs of the *R. sphaeroides* enzyme. This problem can be overcome by the addition of soluble redox mediators as recently shown for the *cbb*₃ enzyme from *B. japonicum* by SERR and electrocatalytic measurements.[39]

The electromagnetic surface enhancement decays with the distance to the substrate in an approximately exponential fashion. For the specific case of heme proteins, however, high-quality SERR spectra can be obtained for separations up to *ca.* 50 Å.

4 Redox and structural equilibria of proteins at interfaces

Electrode–electrolyte interfaces are characterized by an interfacial potential distribution that results in high local electric fields. As an example, the case of an Ag electrode coated with ω-carboxylalkanethiols can be discussed. In a first approach, one can consider a linear potential drop from the positively charged metal up to the negatively charged carboxylate tail groups of the SAM followed by a Guy–Chapman distribution upon entering the bulk solution. Within this approximation, it can be shown that the electric field at the SAM/solution interface, *i.e.* at the protein binding site, is controlled by the difference between the actual potential and the potential of zero charge of the electrode, the charge density at the plane of the carboxylic acid groups and the ionic strength of the electrolyte. The charge density of the SAM in turn is defined by the pK_a of the carboxylic acids in the assembly, which increases with the number of methylene groups, and the pH of the solution. Thus, the electrostatic model predicts electric fields at the protein binding site in the order of 10^8–10^9 V m^{-1} that can be varied by simply changing the length of the alkanethiols without modifying any other parameter.[20] Thicker coatings correspond to lower electric fields.
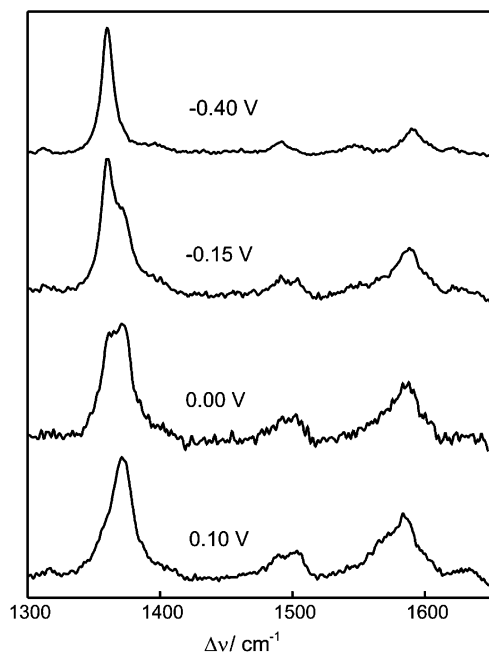
Fig. 4 SERR spectra of cytochrome P450 adsorbed on an Ag electrode coated with mercaptoacetic acid, measured at different potentials.

Fig. 5 Top: 3D structure of Cyt-*c* (PDB 1HRC). Bottom: Redox and structural equilibria of Cyt-*c* in electrostatic complexes.

It is reasonable to expect that fields of this magnitude can be sufficiently strong to affect structural and/or electronic properties of the immobilized proteins. In this respect, SERR represents a unique tool as it is capable of monitoring both aspects simultaneously. This has been shown in a recent study of the soluble tetraheme protein cytochrome c_3 (Cyt-c_3).[29] Electrostatic adsorption of Cyt-c_3 on Ag electrodes coated with mercaptoundecanoic acid occurs without significant structural alterations at the level of the heme groups as inferred from the close similarities of the SERR spectra of the immobilized species and RR spectra in solution. This is confirmed by molecular dynamics simulations which indicate that the same is true for the entire protein. SERR potentiometric titrations, however, indicate that the redox potentials of the four hemes are significantly downshifted with respect to their values in solution, to such an extent that the order of reduction is actually reversed. The experimental results are in excellent agreement with electrostatic calculations. It was concluded that electric fields tend to downshift the redox potentials by stabilizing the ferric form. Indeed, the effect was observed to be more pronounced for the hemes that are closer to the interface, *i.e.* under higher electric fields, according to the docking simulations. This effect is partially compensated by the low dielectric constant of the SAM which tends to shift the redox potentials in the opposite direction.[29]

A similar interplay of effects on the redox potential has been observed for cytochrome P450 immobilized on the same type of electrodes, although in this case the adsorbed protein is almost quantitatively converted into the P420 form as judged from the SERR spectra (Fig. 4).[27]

In contrast, electrostatic adsorption of Cyt-*c* on similar coatings does not appear to have any significant effect on the redox potential but may have distinct structural implications.[20] Specifically, it has been observed that the weak axial iron ligand methionine 80 can detach, yielding a five-coordinated high spin complex (5cHS), and eventually a six-coordinated low spin (6cLS) complex in which the vacant position is occupied by a histidine residue, presumably His26 or His33 (Fig. 5). The component spectra determined for some of the species are shown in Fig. 2.
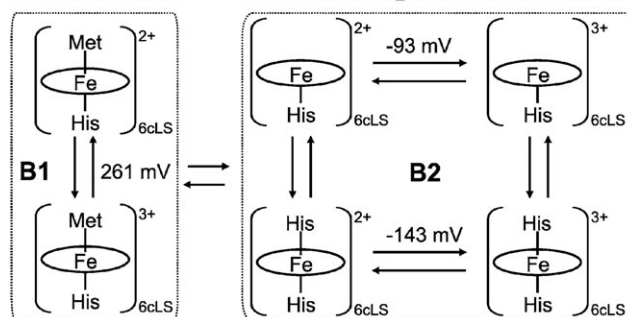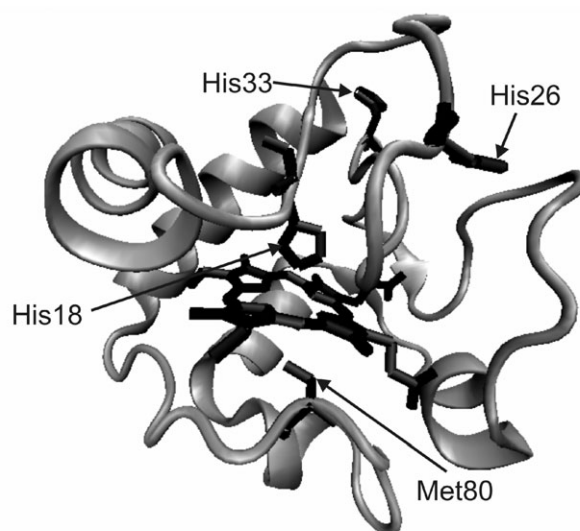
For ferric Cyt-*c* the equilibrium between the native form B1 and the non-native species B2 has been found to sensitively respond to the interfacial electric field. While for ω-carboxyl alkanethiols containing 10 or more methylene residues the B2 contribution is negligible, at shorter tethers, *i.e.* at higher electric fields, it can reach up to *ca.* 75% or even more when the carboxylate groups are replaced by phosphate or sulfate.[11,20] Reduction of the immobilized protein shifts the equilibrium almost quantitatively towards the B1 form independent of the chain length of the SAM.

Similar results have been observed for electrostatic complexes of Cyt-*c* in solution with other model systems such as polyelectrolytes,[35] phospholipid vesicles[12] or, even more relevant, with its natural redox partner cytochrome *c* oxidase.[40] Moreover, also adsorption to hydrophobic surfaces has been found to induce a similar structural equilibrium.[23] Note that detachment of the native axial ligand is associated with a significant downshift of the redox potential (Fig. 5). Detailed spectroscopic studies, including a variety of techniques, have

demonstrated that the B1 → B2 transition occurs without substantial alteration of the protein secondary structure.

5 Electron transfer *vs.* protein dynamics

The kinetics of heterogeneous electron transfer, redox-linked structural changes and other potential-dependent processes can be studied simultaneously by time-resolved (TR) SERR over a broad time scale.[11,19] In this technique the potential-dependent equilibrium of proteins immobilized on a SERR active electrode is suddenly perturbed by a potential jump and the dynamics of relaxation to the new equilibrium at the final potential is monitored by measuring complete SERR spectra at variable delay times. At the end of each perturbation the initial potential of the working electrode is re-established for a sufficiently long time in order to ensure full recovery of the initial equilibrium. The complete cycle is repeated as many times as necessary to achieve a good signal-to-noise ratio. Therefore, the method is restricted to processes that are largely reversible.

In our approach, the duration and amplitude of the potential jumps are controlled by a home-made pulse-delay generator connected to a potentiostat. The same device provides synchronized transistor-transistor logic (TTL) pulses to two consecutive electro-optic laser intensity modulators intercalated in the beam path of a cw laser. In this way, laser pulses of variable duration, down to *ca.* 50 nanosecond, and extinctions better than 10^5 can be easily generated. The detector, a N_2-cooled charge-coupled device of low dark noise, is kept open during the entire measuring cycle. Time resolution is limited by the electrochemical cell constant, which in our case is *ca.* 50–100 microseconds, although it can be improved by miniaturizing the working electrode.[41]

5.1 Distance-dependence of the electron transfer rates

The seminal work by Chidsey *et al.*[42] has inspired the investigation of heterogeneous electron transfer reactions of proteins immobilised on SAM-coated electrodes by electrochemical means and, more recently, by TR-SERR. Thus, several groups have studied the distance-dependence of the electron transfer rates for a variety of proteins immobilized on Au and Ag electrodes coated with pure and mixed SAMs of ω-functionalized alkanethiols. Selected examples are Cyt-*c* on COOH-,[21,43] COOH/OH-,[21,44] CH$_3$-,[21,23] and pyridine-terminated SAMs,[45,46] cytochrome b_{562} on NH$_2$-terminated SAMs,[28] azurin on CH$_3$-terminated SAMs[31] and Cu$_A$ centers on mixed SAMs,[33] among others. A common observation is that for sufficiently long tethers the measured apparent electron transfer rate decays exponentially with increasing number of methylene groups, as expected for long range reactions in which the rate limiting step is electron tunnelling through the alkyl chains (diabatic mechanism). For thinner SAMs, however, the measured rate has been consistently observed to become distance independent. The exact point of demarcation and the absolute values of the measured rates are case-specific. For example, Cyt-*c* on COOH-terminated SAMs gives the expected exponential response for alkanethiols containing 10 or more CH$_2$ groups,[21,43] while for the same protein but coordinatively bound to pyridine-terminated SAMs rates are

faster and the onset is observed at *ca.* 16 CH$_2$ groups.[45,46] The difference is explained in terms of an improved electron pathway in the latter case. However, the question whether this unusual distance dependence obeys a common mechanism or not remains. In fact, different explanations based on qualitatively similar indirect observations have been proposed. Waldeck and co-workers[45,46] suggested that the underlying process is a change of mechanism from a diabatic reaction at long distances to friction-controlled electron transfer at shorter ones. On the other hand, Niki and co-workers[21] proposed that Cyt-*c* adsorbs on COOH-terminated SAMs forming an stable electrostatic complex which is not optimized for electron transfer. Within this two-state model the protein needs to reorient on the surface to a redox-active configuration for electron transfer to take place. This reorientation process, which is assumed to be distance independent, becomes rate limiting at sufficiently short distances due to the exponential increase of the electron tunnelling step.

An intrinsic problem for distinguishing the two proposals is that many of the indirect evidences that support one of the models, *e.g.* viscosity dependence, are also supportive of the other. In this context, we performed TR-SERR experiments utilizing variable potential jumps that correspond to different overpotentials, both for electrostatically and coordinatively bound Cyt-*c*. As expected, the measured electron transfer rate constant for Cyt-*c* electrostatically bound to a long SAM (16-mercaptohexadecanoic acid) shows the expected increase with the driving force for a reaction that is controlled by electron tunnelling. These measurements yield a reorganization energy of *ca.* 0.24 eV, which is significantly lower than the values determined for Cyt-*c* in solution but coincide with independent TR-SERR measurements at constant driving force but as a function of the temperature.[47,48] The difference is ascribed to the exclusion of water molecules from the protein surface and specifically from the region of the partially exposed heme group, and to the reduced dielectric constant at the interface upon electrostatic complexation. In contrast, the apparent electron transfer rate constant of Cyt-*c* bound to short ω-carboxyl alkanethiols, *i.e.* in the plateau region, does not experience any significant change with the applied overpotential (Fig. 6).
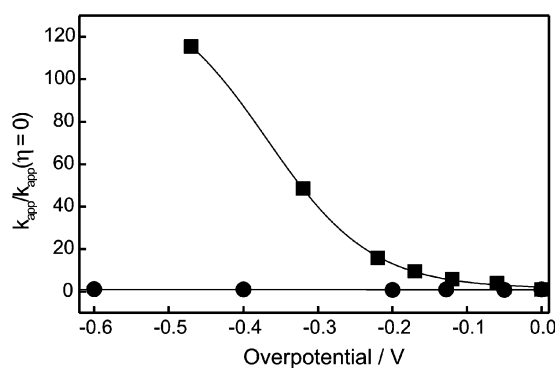
Fig. 6 Overpotential dependence of the apparent electron transfer rates normalized to zero driving force for Cyt-*c* immobilized in two different ways: electrostatically adsorbed on mercaptopropionic acid SAMs (circles) and coordinatively bound to Py-terminated SAM of 6 CH$_2$ groups in length (squares).

The picture emerging from these experiments is that the rate limiting step in the distance independent region is not electron transfer but a different process that precedes the redox reaction, *i.e.* a gated mechanism, at least for electrostatically bound Cyt-*c*.

These results are in sharp contrast with those obtained for Cyt-*c* coordinatively bound to pyridine-terminated SAMs. In this case the apparent electron transfer rate constant, as measured by TR-SERR, shows a strong dependence with the applied overpotential even for the shortest possible monolayer (Fig. 6).[46] Thus, the fact that the rate constant becomes distance independent but remains overpotential dependent provides strong evidence in favour of the friction model proposed by Waldeck and co-workers.[45,46]

5.2 Direct monitoring of the gating step

In the previous section it has been shown that the heterogeneous electron transfer of Cyt-*c* electrostatically bound to electrodes coated with short ω-carboxyl alkanethiols involves a gating step, *i.e.* a preceding process that is rate limiting at sufficiently short distances for which electron tunnelling is expected to be very fast. In order to elucidate the nature of this gating step we have performed SERR experiments using 514 nm excitation.[16] As shown in section 2, SERR measurements at this wavelength are able to provide qualitative information about the average orientation of the protein at the interface. Specifically, variations of the intensity ratio for bands of different symmetry, *e.g.* $\nu_{10}(B_{1g})/\nu_4(A_{1g})$ (see Fig. 1), provide direct evidence of a change of orientation even if the absolute orientation cannot be accurately determined.

Stationary SERR measurements show that the average orientation of the electrostatically immobilized Cyt-*c* depends linearly on the electrode potential and exponentially on the chain length of the ω-carboxyl alkanethiol. Thus, it is expected that the redox reaction is accompanied by protein reorientation as it necessarily implies a change of the electrode potential. TR-SERR experiments demonstrate that this is indeed the case (Fig. 7). At a long SAM, protein reorientation is completed in less than one millisecond as judged from the $\nu_{10}(B_{1g})/\nu_4(A_{1g})$ intensity ratio measured at 514 nm, while electron transfer occurs in a time scale of seconds as probed using 413 nm excitation. In contrast, for a short SAM (6-mercaptohexanoic acid) which is in the plateau region of the distance-dependence plot, both reorientation and electron transfer occur on the same time scale. Moreover, both processes are equally retarded upon increasing the viscosity of the solution or its pH.[16]

Therefore, it is concluded that at short distances the rate limiting step is protein reorientation. This conclusion is further confirmed by the overpotential dependence of the reorientation and electron transfer rate constants of Cyt-*c* adsorbed on a 11-mercaptoundecanoic acid SAM, *i.e.* at the point of change in the distance-dependent plots of the apparent electron transfer rates. For jumps to the redox potential reorientation is significantly faster than electron transfer and thus the overall rate is controlled by electron tunnelling. Upon increasing the overpotential the apparent electron transfer rate increases but only up to the point that it coincides with the
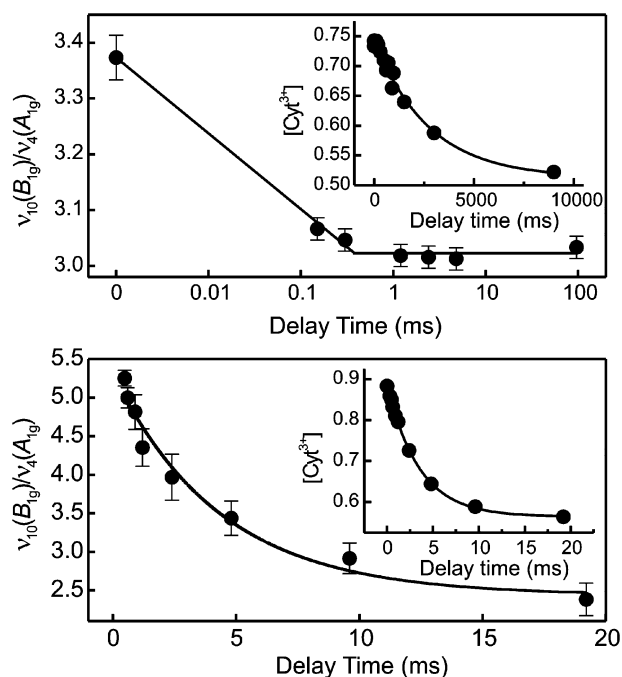
Fig. 7 Time evolution of the $\nu_{10}(B_{1g})/\nu_4(A_{1g})$ intensity ratio measured with 514 nm excitation for ferric Cyt-*c* adsorbed on electrodes coated with mercaptohexadecanoic acid (top) and mercaptohexanoic acid (bottom). The insets show the reduction processes as followed by TR-SERR at 413 nm. All experiments refer to potential jumps from 50 to −50 mV.

reorientation rate which is independent of the final potential in the TR-SERR experiments.[16]

In summary, Cyt-*c* adsorbs on negatively charged surfaces with an orientation that, although coarsely predetermined by the patch of lysines around the partially exposed heme, depends in its details on the strength of the interactions. Shorter SAMs provide a larger charge density at the interface and, therefore, a larger electric field that affects the average equilibrium orientation at each potential. The equilibrium average orientation does not necessarily provide an efficient electron pathway. Thus, the overall electron transfer rate will depend on the interplay between electron tunnelling probabilities and mobility (reorientation) of the protein at the surface. At long distances and low electric fields reorientation is very fast (>6000 s^{-1} for mercaptohexadecanoic acid) while electron tunnelling is very slow and, therefore, rate limiting. At shorter distances, *i.e.* at higher electric fields, the activation energy for reorientation is significantly larger, limiting the motion of the protein at the surface. Thus, although the tunnelling pathway through the SAM is shorter, the probability that the protein finds an orientation that provides a good electronic coupling becomes limiting.

5.3 Structural dynamics

As shown in section 3, electrostatic and hydrophobic interactions of Cyt-*c* with model systems, including the natural reaction partner cytochrome *c* oxidase and SAM-coated electrodes, leads to a conformational equilibrium between the native form B1 and another state, B2, which lacks the axial
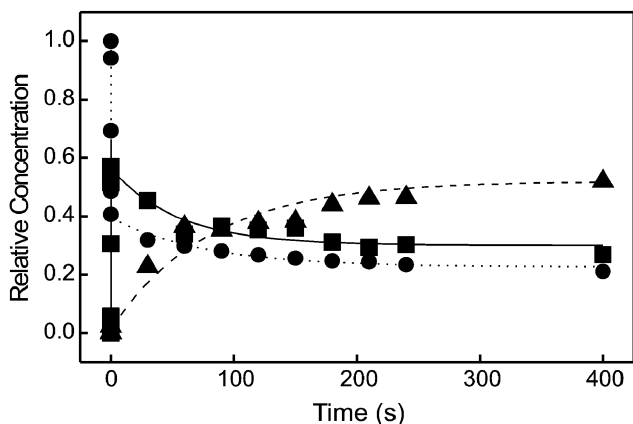
Fig. 8 Electron transfer and structural changes of Cyt-*c* adsorbed on an mercaptopropanoic acid-coated electrode after an oxidative potential jump. Circles: native ferrous (B1). Squares: native ferric (B1). Triangles: non-native (B2) ferric.

ligand Met-80 (Fig. 5). High electric fields shift the equilibrium towards the B2 form. However, the B1 → B2 conversion proceeds very slowly under these conditions, as probed by TR-SERR. As shown in Fig. 8, for a short SAM (mercaptopropanoic acid), a potential jump from a sufficiently negative potential to the redox potential results in a fast oxidation of the native adsorbed Cyt-*c* followed by the formation of the B2 species in a much longer time scale.[10]

In contrast, for Cyt-*c* adsorbed on hydrophobic SAMs, *i.e.* at low electric fields, the conformational transition occurs almost instantaneously after oxidation (*ca.* 10^5 s^{-1}).[23]

6 Conclusions and outlook

SERR spectroscopy represents a powerful tool for studying proteins immobilized on metallic substrates, such as electrodes. The kind of information that it provides is not restricted to Faradaic processes, as in traditional electrochemical methods, but it provides simultaneously structural and orientational parameters over a wide dynamic range. Furthermore, it facilitates the investigation of proteins containing multiple redox centers that are not easily distinguished by other methods.

This kind of information is of crucial interest for the rational design and improvement of protein-based devices such as sensors, enzymatic nanoreactors and biofuel cells. On the other hand, SERR studies of redox proteins attached to biomimetic surfaces may provide a deeper insight into the parameters that govern the functioning of these molecules under physiological conditions. For example, based on the SERR studies of Cyt-*c* on Ag electrodes coated with COOH-terminated SAMs summarized in the preceding sections, the following potential implications can be derived for the functioning of this electron transporter. Let us consider the electron transfer reaction between Cyt-*c* and the corresponding oxidase embedded into the mitochondrial membrane (Fig. 9). The first step is the formation of an electrostatic complex *via* the positively charged patch of Cyt-*c* around the partially exposed redox center and the negatively charged domain of the oxidase. This electrostatic complex is not necessarily optimized for electron transfer from Cyt-*c* to the Cu$_A$ primary acceptor of the enzyme. Thus, the second step of the mechanism may imply the reorganization of the electrostatic complex. If the local electric field is sufficiently low this reorganization will proceed rapidly leading to efficient electron tunnelling. The charge transfer reaction is fast despite the long distance and extremely low driving force (close to 0 eV) due to the lowering of the reorganization energy in the electrostatic complex, as suggested from TR-SERR experiments on the model systems. However, the fact that the driving force for the forward redox reaction is nearly zero implies that back electron transfer may eventually compete efficiently. On the other hand, oxidation of Cyt-*c* at low electric fields may trigger a fast conformational transition to the state B2 whose redox potential is sufficiently downshifted to prevent re-reduction of the carrier. The final step would be the dissociation of Cyt-*c* from the binding site which rapidly returns to the B1 form in solution. Such a mechanism would guarantee an efficient and unidirectional inter-protein reaction.
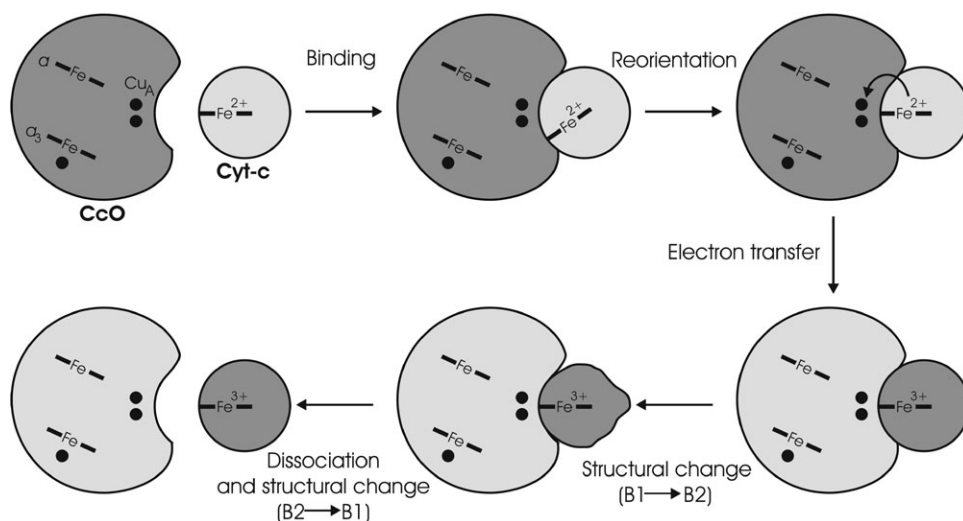
Fig. 9 Schematic representation of the electron transfer reaction between Cyt-*c* and cytochrome *c* oxidase (C*c*O).

The variable component of the electric field at the mitochondrial membrane is mainly associated with the translocation of protons across the membrane along the electroprotonic energy transduction chain. This proton gradient is in turn converted into chemical energy by ATP-synthase. Thus, a mismatch between the production of the proton gradient and its consumption may result in an increase of the electric field. Such an increase might be sufficient to block the reorganization of the initial Cyt-c/enzyme complex and the B1 → B2 transition of Cyt-c preventing electron transfer and, therefore, unproductive proton translocation by the oxidase. Thus, it is hypothesised that the electric field regulation of Cyt-c dynamics and structure may play a crucial role in regulating mitochondrial respiration.

These conclusions are far from being fully proven and simply constitute a reasonable working hypothesis based on the results of SERR experiments with simple model systems. Further studies with more realistic model systems, including protein–protein complexes, are required and certainly SERR spectroscopy will play a crucial role in these investigations.

Acknowledgements

References

1 J. R. Ferraro, K. Nakamoto and C. W. Brown, *Introductory Raman Spectroscopy*, Academic Press, San Diego, CA, 2nd edn, 2003.
2 A. C. Albrecht, *J. Chem. Phys.*, 1961, **34**, 1476.
3 T. Kitagawa and Y. Mizutani, *Coord. Chem. Rev.*, 1994, **135**, 685.
4 T. G. Spiro, *Adv. Protein Chem.*, 1985, **37**, 111.
5 A. Desbois, *Biochimie*, 1994, **76**, 693.
6 S. Z. Hu, I. K. Morris, J. P. Singh, K. M. Smith and T. G. Spiro, *J. Am. Chem. Soc.*, 1993, **115**, 12446.
7 T. M. Cotton, S. G. Schultz and R. P. Van Duyne, *J. Am. Chem. Soc.*, 1980, **102**, 7960.
8 R. Aroca, *Surface-Enhanced Vibrational Spectroscopy*, John Wiley & Sons, Ltd., Chichester, 2006.
9 D. Murgida and P. Hildebrandt, Surface-Enhanced Raman Scattering: Physics and Applications, *Top. Appl. Phys.*, 2006, **103**, 313.
10 D. H. Murgida and P. Hildebrandt, *Phys. Chem. Chem. Phys.*, 2005, **7**, 3773.
11 D. H. Murgida and P. Hildebrandt, *Acc. Chem. Res.*, 2004, **37**, 854.
12 S. Oellerich, H. Wackerbarth and P. Hildebrandt, *J. Phys. Chem. B*, 2002, **106**, 6566.
13 S. Dopner, P. Hildebrandt, A. G. Mauk, H. Lenk and W. Stempfle, *Spectrochim. Acta, Part A*, 1996, **52**, 573.
14 *Surface-enhanced Raman Scattering*, ed. K. Kneipp, M. Moskovits, H. Kneipp, Springer, Berlin, 2006, vol. 103.
15 I. D. G. Macdonald and W. E. Smith, *Langmuir*, 1996, **12**, 706.
16 A. Kranich, H. K. Ly, P. Hildebrandt and D. H. Murgida, unpublished work.
17 G. Smulevich and T. G. Spiro, *J. Phys. Chem.*, 1985, **89**, 5168.
18 A. M. Kuznetsov and J. Ulstrup, *Electron Transfer in Chemistry and Biology. An Introduction to the Theory*, John Wiley & Sons Ltd., Chichester, 1999.
19 D. H. Murgida and P. Hildebrandt, *Angew. Chem., Int. Ed.*, 2001, **40**, 728.
20 D. H. Murgida and P. Hildebrandt, *J. Phys. Chem. B*, 2001, **105**, 1578.
21 A. Avila, B. W. Gregory, K. Niki and T. M. Cotton, *J. Phys. Chem. B*, 2000, **104**, 2759.
22 M. J. Tarlov and E. F. Bowden, *J. Am. Chem. Soc.*, 1991, **113**, 1847.
23 L. Rivas, D. H. Murgida and P. Hildebrandt, *J. Phys. Chem. B*, 2002, **106**, 4823.
24 D. H. Murgida and P. Hildebrandt, *J. Mol. Struct.*, 2001, **565**, 97.
25 J. J. Wei, H. Y. Liu, A. R. Dick, H. Yamamoto, Y. F. He and D. H. Waldeck, *J. Am. Chem. Soc.*, 2002, **124**, 9591.
26 D. H. Murgida, P. Hildebrandt, J. Wei, Y. F. He, H. Y. Liu and D. H. Waldeck, *J. Phys. Chem. B*, 2004, **108**, 2261.
27 S. Todorovic, C. Jung, P. Hildebrandt and D. H. Murgida, *JBIC, J. Biol. Inorg. Chem.*, 2006, **11**, 119.
28 T. Albrecht, PhD Thesis, Technische Universität Berlin, 2003.
29 L. Rivas, C. M. Soares, A. M. Baptista, J. Simaan, R. Di Paolo, D. H. Murgida and P. Hildebrandt, *Biophys. J.*, 2005, **88**, 4188.
30 A. Kranich, M. A. De la Rosa, P. Hildebrandt and D. H. Murgida, unpublished work.
31 Q. J. Chi, J. D. Zhang, J. E. T. Andersen and J. Ulstrup, *J. Phys. Chem. B*, 2001, **105**, 4669.
32 G. N. Ledesma, D. H. Murgida, H. K. Ly, H. Wackerbarth, J. Ulstrup, A. J. Costa and A. J. Vila, *J. Am. Chem. Soc.*, 2007, **129**, 11884.
33 K. Fujita, N. Nakamura, H. Ohno, B. S. Leigh, K. Niki, H. B. Gray and J. H. Richards, *J. Am. Chem. Soc.*, 2004, **126**, 13954.
34 J. Grochol, R. Dronov, F. Lisdat, P. Hildebrandt and D. H. Murgida, *Langmuir*, 2007, **23**, 11289.
35 I. M. Weidinger, D. H. Murgida, W. F. Dong, H. Mohwald and P. Hildebrandt, *J. Phys. Chem. B*, 2006, **110**, 522.
36 J. J. Feng, P. Hildebrandt and D. H. Murgida, *Langmuir*, 2008, **24**, 1583.
37 S. Todorovic, M. M. Pereira, T. M. Bandeiras, M. Teixeira, P. Hildebrandt and D. H. Murgida, *J. Am. Chem. Soc.*, 2005, **127**, 13561.
38 J. Hrabakova, K. Ataka, J. Heberle, P. Hildebrandt and D. H. Murgida, *Phys. Chem. Chem. Phys.*, 2006, **8**, 759.
39 S. Todorovic, A. Verissimo, N. Wisitruangsakul, P. Hildebrandt, M. M. Pereira, M. Teixeira and D. H. Murgida, unpublished work.
40 S. Döpner, P. Hildebrandt, F. I. Rosell, A. G. Mauk, M. von Walter, G. Buse and T. Soulimane, *Eur. J. Biochem.*, 1999, **261**, 379.
41 A. J. Bard and L. R. Faulkner, *Electrochemical Methods. Fundamentals and Applications*, John Wiley & Sons Inc., Hoboken, 2nd edn, 2001.
42 C. E. D. Chidsey, *Science*, 1991, **251**, 919.
43 D. H. Murgida and P. Hildebrandt, *J. Am. Chem. Soc.*, 2001, **123**, 4062.
44 T. D. Dolidze, S. Rondinini, A. Verto-Va, D. H. Waldeck and D. E. Khoshtariya, *Biopolymers*, 2007, **87**, 68.
45 J. J. Wei, H. Y. Liu, D. E. Khoshtariya, H. Yamamoto, A. Dick and D. H. Waldeck, *Angew. Chem., Int. Ed.*, 2002, **41**, 4700.
46 H. J. Yue, D. Khoshtariya, D. H. Waldeck, J. Grochol, P. Hildebrandt and D. H. Murgida, *J. Phys. Chem. B*, 2006, **110**, 19906.
47 D. H. Murgida and P. Hildebrandt, *J. Phys. Chem. B*, 2002, **106**, 12814.
48 P. Hildebrandt and D. H. Murgida, *Bioelectrochemistry*, 2002, **55**, 139.